UNIVERSITY OF OSLO

INF5410 Array signal processing. Ch. 3: Apertures and Arrays, part II

Andreas Austeng

Department of Informatics, University of Oslo

February 2010

UNIVERSITY OF OSLO

Outline

UNIVERSITY OF OSLO

Periodic spatial sampling in one dimension

- Array:
  - Consists of individual sensors that sample the environment spatially
  - Each sensor could be an aperture or omni-directional transducer
  - Spatial sampling introduces some complications (Nyquist sampling, folding, . . .)
- Question to be asked/answered:
  When can $f(x, t_0)$ be reconstructed by $\{y_m(t_o)\}$?
  - $f(x, t)$ is the continuous signal and
  - $\{y_m(t)\}$ is a sequence of temporal signals where $y_m(t) = f(md, t)$, d being the spatial sampling interval.

UNIVERSITY OF OSLO

Periodic spatial sampling in one dimension ...

- Sampling theorem (Nyquist):
  If a continuous-variable signal is band-limited to frequencies below k_0, then it can be periodically sampled without loss of information so long as the sampling period $d \leq \pi/k_0 = \lambda_0/2$.

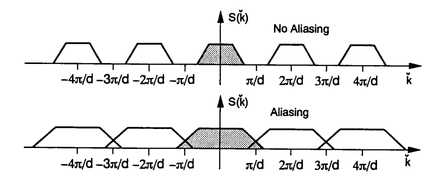

Figure 3.13 The periodic spectrum $S(\tilde{k})$ is equal to the sum of periodic replications of the spectrum $S_c(k)$. In this case the periodic replications do not overlap because $S_c(k)$ is bandlimited to a frequency $k_0 \leq \pi/d$. When the spectrum $S_c(k)$ is not bandlimited to frequencies below π/d, one period of the periodic spectrum $S(\tilde{k})$ does not equal $S_c(k)$. This phenomenon is called *aliasing*.

Periodic spatial sampling in one dimension ...

- Periodic sampling of one-dimensional signals can be straightforwardly extended to multidimensional signals.
- "Rectangular / regular" sampling not necessary for multidimensional signals.

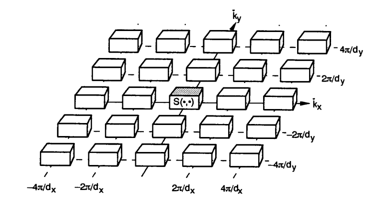

Figure 3.14 $S(\hat{k}_x, \hat{k}_y)$ can be interpreted as the periodic extension of $S_c(k_x, k_y)$. When $s_c(x, y)$ is bandlimited and the sampling intervals d_x and d_y are chosen small enough (as shown here), $s_c(x, y)$ may be reconstructed from the samples $s(m, n)$.

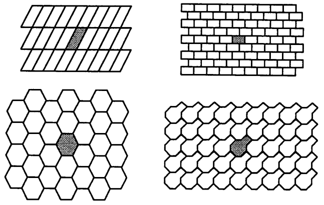

Figure 3.16 Several differently shaped baseband regions $\Re$, when periodically extended in a manner consistent with Cartesian sampling, completely cover the two-dimensional frequency plane.

Regular arrays

- Assume point sources ($W_{tot} = W_{array} \cdot W_{el}$)).
- Easy to analyze and fast algorithms available (FFT).

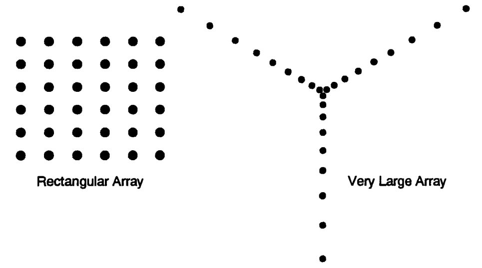

Figure 3.17 Two arrays of discrete sensors are shown. On the left, rectangular array has periodically spaced sensors. The *VLA* shown on the right has power-law spaced sensors along each arm (see Prob. 3.16).

Regular arrays; linear array

- Consider linear array; M equally spaced ideal sensor with inter-element spacing d along the x direction.
  - The discrete aperture function, w_m.
  - The discrete aperture smoothing function, $W(k)$:

    $$W(k) \equiv \sum_m w_m e^{\jmath kmd}$$

  - Spatial aliasing given by d relative to λ.

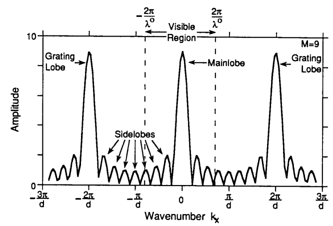

Figure 3.20 The aperture smoothing function magnitude $|W(k)|$ for uniform shading is plotted for a nine-sensor regular linear array. This spatial spectrum has period $k = 2\pi/d$. The visible region of the aperture smoothing function is that part for which $-2\pi/\lambda^o \le k_x^o \le 2\pi/\lambda^o$. What might be called secondary mainlobes—those not located at the origin—are termed grating lobes.

Grating lobes

- Given an linear array of M sensors with element spacing d.
  - $W(k) = \frac{\sin kMd/2}{\sin kd/2}$.
  - Mainlobe given by $D = Md$.
  - Gratinglobes (if any) given by d.
  - Maximal response for $\phi = 0$. Does it exist other ϕ_g with the same maximal response?
    $k_x = 2\frac{\pi}{\lambda}\sin\phi_g \pm 2\frac{\pi}{d}n \Rightarrow \sin\phi_g = \pm\frac{\lambda}{d}n$.
  - $n = 1$: No gratinglobes for $\lambda/d > 1$, i.e. $d < \lambda$.
  - $d = 4\lambda$:
    $\sin\phi_g \pm n \cdot 1/4 \Rightarrow \phi_g = \pm 14.5^\circ, \pm 30^\circ, \pm 48.6^\circ, \pm 90^\circ$.

Element response

- If the elements have finite size:

$$W_e(\vec{k}) = \int_{-\infty}^{\infty} w(\vec{k}) e^{j\vec{k}\cdot\vec{x}} d\vec{x}$$

  - If linear array:
    Continuous aperture “devided into” M parts of size d
    Each single element: $\frac{sin(kd/2)}{k/2} \rightarrow$ first zero at $k = 2\pi/d$
- Total response:
  $W_{\text{total}}(\vec{k}) = W_e(\vec{k}) \cdot W_a(\vec{k})$,
  where $W_a(\vec{k})$ is the array response when point sources are assumed.

Irregular arrays

- Discrete co-array function:
  - $c(\vec{\chi}) = \sum_{(m_1,m_2)\in\vartheta(\vec{\chi})} w_{m_1} w^*_{m_2}$, where $\vartheta(\vec{\chi})$ denotes the set of indices (m_1, m_2) for which $\vec{x}_{m_2} - \vec{x}_{m_1} = \vec{\chi}$.
  - $0 \leq c(\vec{\chi}) \leq M = c(\vec{0})$.
  - Equals the inverse Fourier Transform of $|W(\vec{k})|^2$
    $\Rightarrow$ sample spacing in the lag-domain must be small enough to avoid aliasing in the spatial power spectrum.
  - Redundant lag: The number of distinct baselines of a given length is grater than one.

Examples

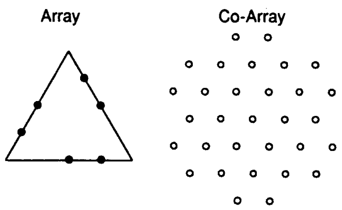

Figure 3.22 The Haubrich array shown on the left has the co-array on the right. Because there are no redundant baselines in the array, the co-array values are all equal to one except at the origin (zero lag), where the co-array value is M.

Examples ...

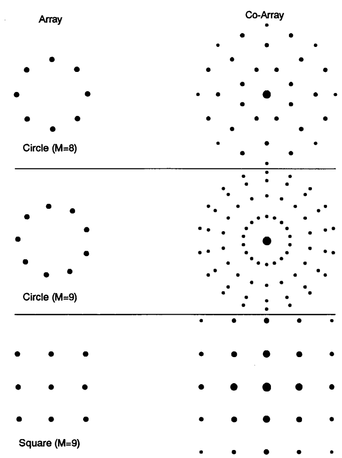

Figure 3.23 The sensor locations for two circular arrays and a square array are shown in the left column. The first of the circular arrays contains eight sensors; the square array and the remaining circular array each contain nine sensors. Their corresponding co-arrays are shown in the right column. The area of the circles denoting co-array locations is proportional to the redundancy at that lag. The redundancy at the origin of a co-array always equals M. Note how these regular array geometries lead to co-arrays spanning complicated spatial regions.

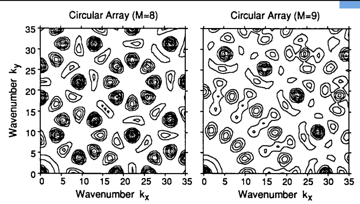

Figure 3.25 The panels depict the Fourier Transforms of the co-arrays for the circular arrays depicted in Fig. 3.23. The computations for the eight-sensor array are shown on the left, the nine-sensor on the right. The spectra are plotted only over the first quadrant of wavenumber space. Peak height can be judged by the number of contours encircling the peak.

Irregular arrays

- Sparse arrays
  - Underlying regular grid, all position not filled.
  - Position fills to acquire a given co-array
    - Non-redundant arrays with minimum number of gaps
    - Maximal length redundant arrays with no gaps.
  - Sparse array optimization
    - Irregular arrays can give regular co-arrays ...

Examples

- Non-redundant arrays == Minimum hole arrays == Golumb arrays *1101*, *1100101*, *110010000101*
- Redundant arrays == Minimum redundancy arrays *1101*, *1100101*, *1100100101*

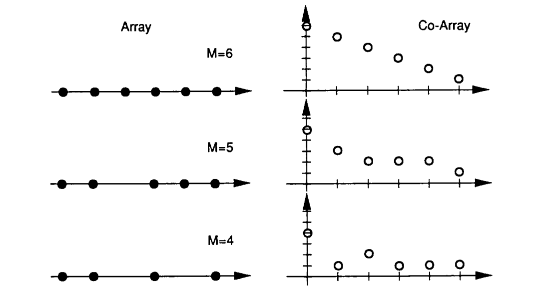

Figure 3.27 A six-sensor, filled array and its co-array are shown. Two arrays having the same aperture are derived by successively removing sensors from the array. This thinning procedure results in the depicted co-arrays. To derive the four-sensor perfect array, one must start with a seven-sensor filled array.

Random arrays

- $W(\vec{k}) = \sum_{m=0}^{M-1} e^{\jmath \vec{k}\cdot\vec{x}_m}$ (assumes unity weights)
- $E[W(\vec{k})] = \sum_{m=0}^{M-1} E[e^{\jmath \vec{k}\cdot\vec{x}_m}] = M \int p_x(\vec{x}_m) e^{\jmath \vec{k}\cdot\vec{x}_m} d\vec{x} = M \cdot \Phi_x(\vec{k})$
  i.e. Equals the array pattern of a continuous aperture where the probability density function plays the same role as the weighting function.
- $var[W(\vec{k})] = E[|W(\vec{k})|^2] - (E[W(\vec{k})])^2$
  - $E[|W(\vec{k})|^2] = E[\sum_{m_1=0}^{M-1} e^{\jmath \vec{k}\cdot\vec{x}_{m_1}} \cdot \sum_{m_2=0}^{M-1} e^{-\jmath \vec{k}\cdot\vec{x}_{m_2}}]$
    $= E[M \cdot 1 + \sum_{m_1, m_1 \neq m_2} e^{\jmath \vec{k}\cdot\vec{x}_{m_1}} \cdot \sum_{m_2} e^{-\jmath \vec{k}\cdot\vec{x}_{m_2}}]$
    Assumes uncorrelated x_m $(E[x \cdot y] = E[x] \cdot E[y])$
    $\Rightarrow E[|W(\vec{k})|^2] = M + (M^2 - M)|\Phi_x(\vec{k})|^2$

  $\Rightarrow var[W(\vec{k})] = M - M|\Phi_x(\vec{k})|^2$